ENGINEERING TRANSACTIONS • *Engng. Trans.* • **61**, 1, 65–80, 2013
Polish Academy of Sciences • Institute of Fundamental Technological Research (IPPT PAN)
National Engineering School of Metz (ENIM)

An Experimental Investigation and Modelling of Friction Stir Processing

Marek Stanisław WĘGLOWSKI[1)], Carter Benjamin HAMILTON[2)]

[1)] *Institute of Welding (Instytut Spawalnictwa)*
Błogosławionego Czesława 16-18, 44-100 Gliwice, Poland
e-mail: marek.weglowski@is.gliwice.pl

[2)] *Miami University, School of Engineering and Applied Science*
Oxford 45056, Ohio, USA

In this paper experimental and numerical modelling of the Friction Stir Processing technique are presented. The experiments were carried out on cast aluminium alloy AlSi9Mg. A conventional tool without a pin was used. During the trials, the tool temperature, torque and forces acting on the tool were measured. The results revealed that an increase in the rotational speed caused an increase in the temperature and a decrease in the torque. Furthermore, the increase in travelling speed caused a decrease in the tool temperature and an increase in the torque. The experimental results were compared with that achieved based on the numerical modelling.

Key words: Friction Stir Processing, aluminium alloys, modelling.

1. Introduction

Friction Stir Processing (FSP), based on the stir of material, utilizes the same process principles as FSW (Friction Stir Welding) [1]; however, instead of joining samples together, the process modifies the local microstructure of monolithic specimens to achieve specific and desired properties by surface modifying the microstructure (Fig. 1a). As in FSW, the tool induces plastic flow during the process, but depending on the selection of process parameters, i.e. applied force, travelling speed and rotational speed, the material flow can yield a modified microstructure that is beneficial to the performance/requirement of the material. Developed by Mishra in 2000, the modified process is a new and exciting technique for microstructural development and modification as well as property enhancement [2].

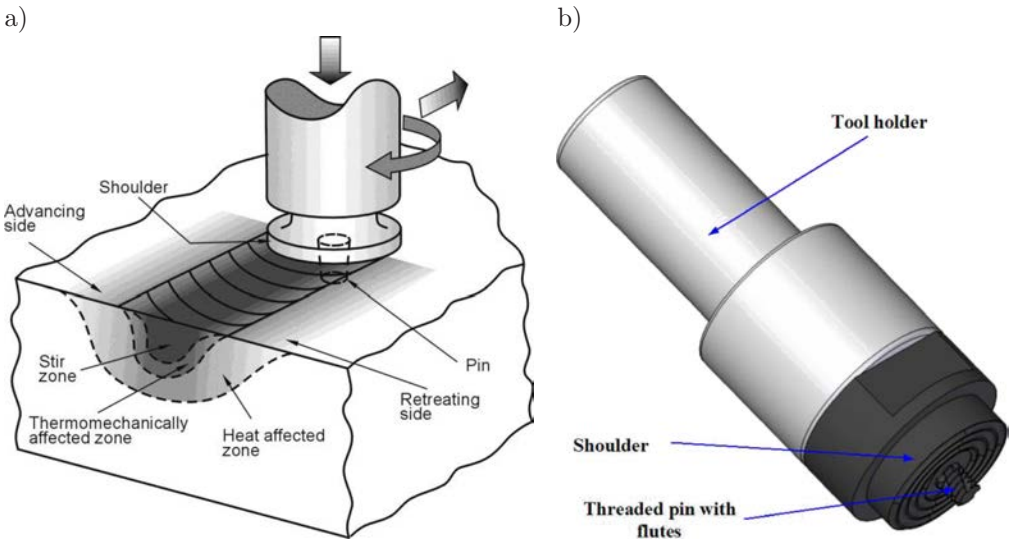

FIG. 1. Schematic drawing of Friction Modified Processing technique a) and tool b).

Friction stir welding is an energy-efficient, environmental-friendly and versatile joining technology that delivers superior strength, corrosion resistance and fatigue resistance when compared to conventional welding methods [2]. Developed and patented in 1991 [1] by The Welding Institute (TWI) – the United Kingdom, friction stir welding is a novel solid-state joining process that continues to gain popularity in the manufacturing sector [2, 3]. Prominent examples of FSW application include EADS/Airbus' utilization of friction stir welding to join aluminium components on the new A400M transport aircraft and Lockhead-Martin Michoud's use of FSW to join aluminium panel sections of the Space Shuttle's external fuel tank. Utilizing a rotating tool design, FSW induces plastic flow in the base materials and effectively stirs (or extrudes) the workpieces together. Since no melting occurs during FSW, the process is performed at much lower temperatures than conventional welding techniques and circumvents many of the environmental and safety issues associated with these welding methods. FSW produces a welded joint that is fundamentally defect-free and that displays excellent mechanical properties when compared to liquid state welds [3–5]. Due to these benefits, industries are embracing FSW technology and implementing new welding capabilities into their manufacturing sectors.

During the FSP process, a pin is plunged into the material with the shoulder of the rotating tool abutting the base metals (a tool without a pin can also be used). As the tool (Fig. 1) transverses the modified direction, the rotation of the shoulder under the influence of an applied load heats the metal surrounding the modified area and with the rotating action of the pin/shoulder induces

metal from each section to flow and form the modified area. The microstructure that evolves during FSP results from the influence of material flow, plastic deformation and elevated temperature and is characterized by a central stir zone surrounded by a thermomechanically affected zone (TMAZ) and heat affected zone (HAZ) as shown in Fig. 1. On the "advancing side" (Fig. 1) of the modified area, rotation of the tool is in the same direction as the modified direction, but on the "retreating side" (Fig. 1), rotation of the tool is in the opposite direction of the modified direction. In the FSP process the most important area is between the stir zone and the thermomechanically affected zone. This area will determine the properties of modified area, especially adhesion. In FSW the most important area is the stir zone, a key difference between the FSP and FSW processes. The second difference is that for FSP another critical area is the zone directly below the pin. This is less critical for FSW, which is concerned with the weld/joint quality throughout the thickness of the workpieces.

Numerous investigations have sought to characterize and model the FSW process, and the current status of friction stir research has been summarized well by Mishra [2] and Ma [6]. Friction Stir Processing involves complex processes such as flow of material, temperature distribution, rotary forces, tool design etc. that are not fully understand.

Although several numerical models of friction stir welding have been developed for the calculation of the heat generation rate [7, 8] and heat transfer and materials flow [7, 9], their testing has, for most part, been limited to the comparison of the numerically predicted temperatures *versus* time plots with the corresponding experimental data. A rigorous validation of numerical models must include examination of the model's capability to predict several important features of the friction processing such as the torque, temperature, power needed for modification and the geometry of the stir zone as a function of important process parameters over a wide range of values.

In this paper the results of experimental trials and numerical modelling are presented. The main goal of this investigation was to determine the relationship between the process parameters of Friction Stir Processing and the torque acting on the tool and the temperature of the tool.

2. Experimental procedure

The chemical composition of the AlSi9Mg cast aluminium alloy used in this study is provided in Table 1. The base metal microstructure consists of oarse acicular Si particles distributed along the primary aluminium dendrite boundaries. Furthermore, the material exhibited numerous pores as shown in Fig. 2. Test plates were prepared from 6 mm thick plate with dimensions of 400 mm in length and 100 mm in width. Prior to tests, each plate was milled on both

Table 1. Chemical composition of cast aluminium alloy AlSi9Mg acc. to EN 1706 [10].

Chemical composition [%] mass							
Si	Fe	Cu	Mn	Mg	Zn	Ti	Al
9.0–10.0	0.19	0.05	0.10	0.25–0.45	0.07	0.15	balance

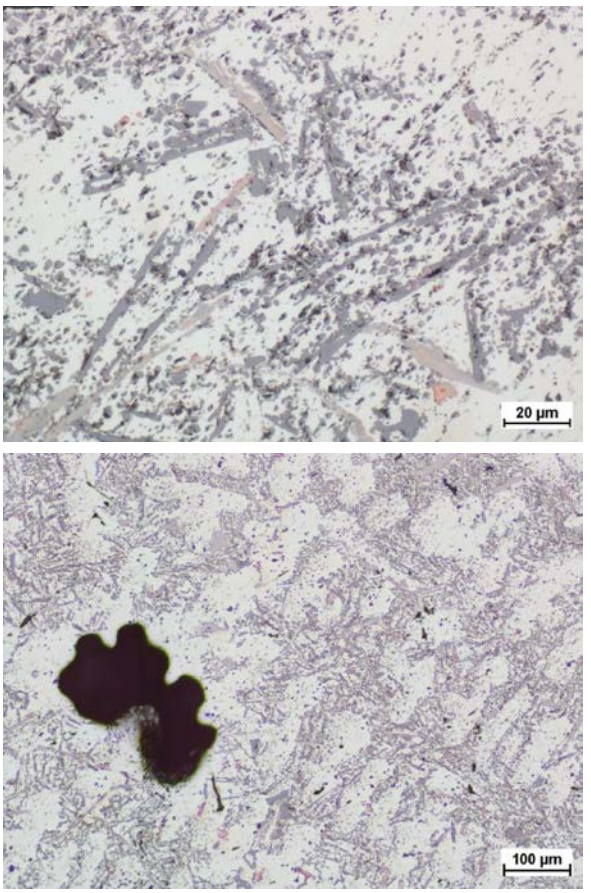

FIG. 2. Microstructure of parent material, cast aluminium alloy AlSi9Mg, light microscop.

sides to remove roughness as a result of casting. The plates, however, were not cleaned before experimentation.

A conventional tool with a scrolled shoulder (20 mm in diameter) and no pin was used for all the trials. The shoulder of the tool is manufactured from high speed tool steel -HS6-5-2. The geometry of the tool is shown in Fig. 3. A 0.5-deg head tilt was applied during plunge and FSP trials. Trials were conducted to determine the working range of rotation and travelling speeds. Thirty experimental conditions were taken into consideration (Fig. 4).

FIG. 3. The geometry of the FSP tool.

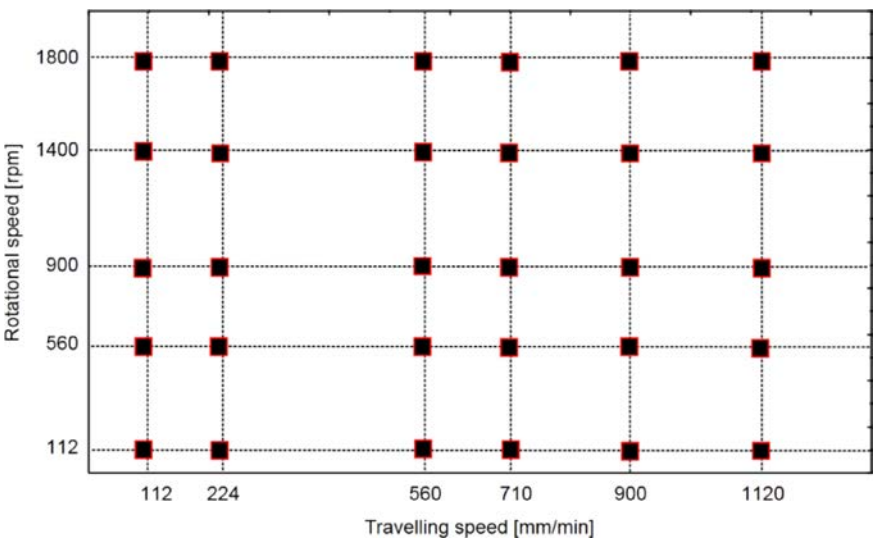

FIG. 4. Range of parameters utilised during experiments.

Transverse samples were removed from the modified plates for light metallographic analysis. Each sample was ground, polished through 1 μm diamond paste and final polished with a 0.25 μm Al_2O_3 suspension. Samples were analysed optically at magnifications up to 500× using a Nikon Eclipse MA 200 microscope without etching.

The TermSTIR device recorded the temperature of the tool. The variations in temperature during the processing were measured by a K-type thermocouple inserted to a place located 1.0 mm away from the tip of the rotating tool shoulder. The temperature of the tool was measured at 60 Hz of frequency. The mean value of the spindle torque, vertical force and down force were measured by the LOWSTIR head and calculated from 100 points in the area of the fully stabilized FSP process (Fig. 5) at a sampling rate of 100 Hz. It should be emphasized that the signals recorded during FSP are characteristic for the specific

tool geometry, parameters of the process, base material, measurement system (LOWSTIR) and experimental setup.

3. Results and discussion

3.1. Experimental results of measurements

Data of torque and temperature for the changes of rotational and travelling speeds are shown in Figs. 5 to 8. As has been generally observed [11] increasing the rotational speed rapidly decreases the torque acting on the tool, as can be seen in Fig. 5. This is caused by the well-known phenomena for friction welding (rotary) in which an increase of the rotational speed causes a decrease in the torque [12] and the thickness of stir material layer [13]. In the FSP process the increase in rotational speed causes the volume of modified (stir) material to also become lower. And at this smaller volume the rotating tool generates a high amount of heat. Thus the temperature increases for increasing rotational speeds (Fig. 6) and causes the friction coefficient to decrease. Therefore, the "resistance" of the material becomes lower, thereby reducing the torque. An empirical relationship was developed to describe the relationship between torque and rotational speed. The evaluation of the rotational speed affecting the temperature of the modified material was successfully approximated by linear functions. The results of mathematical modelling for torque and for temperature are given in Tables 2 and 3, respectively.

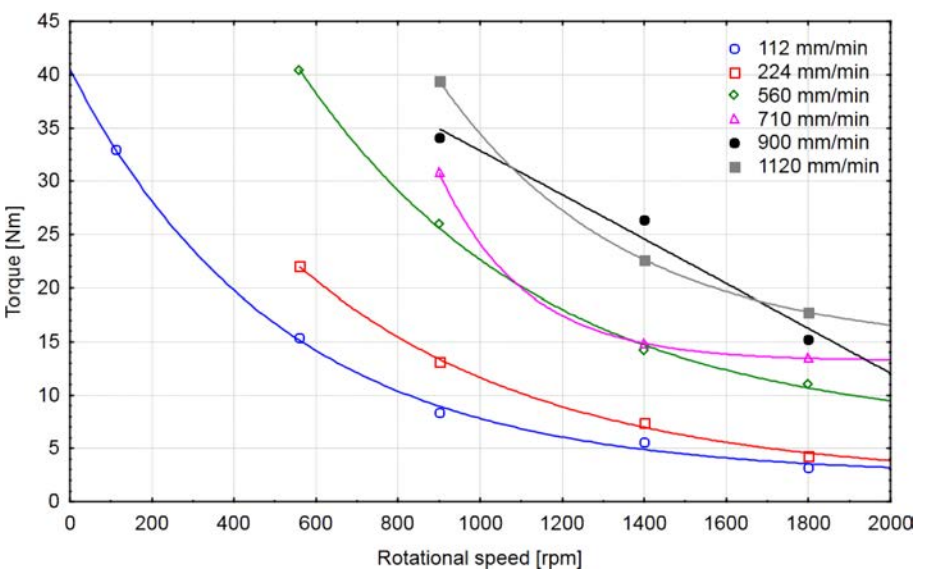

Fig. 5. Influence of the rotational speed on the torque acting on the tool at constant travelling speed.

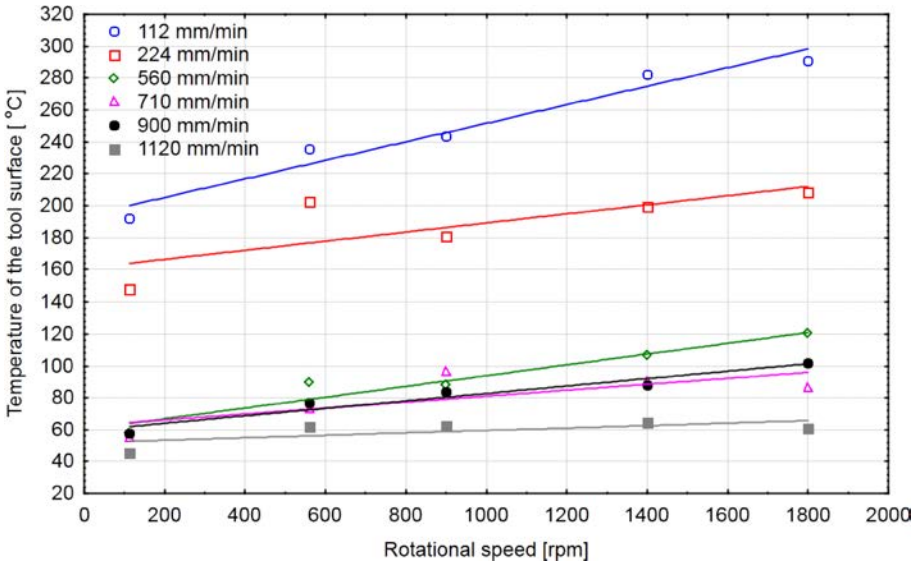

FIG. 6. Influence of rotational speed on tool temperature at constant travelling speed.

Table 2. The mathematical relationship between rotational speed (ω) and torque acting on the tool (M) at constant travelling speed (v).

No.	v [mm/min]	Models
1	112	$M_{112} = 38.01 \cdot \exp(-\omega/509.78) + 2.46$
2	224	$M_{224} = 50.75 \cdot \exp(-\omega/600.77) + 2.04$
3	560	$M_{560} = 87.74 \cdot \exp(-\omega/590.46) + 6.51$
4	710	$M_{710} = 1265.79 \cdot \exp(-\omega/210.45) + 13.22$
5	900	$M_{900} = -1049.18 \cdot \exp(\omega/51865.59) + 1102.48$
6	1120	$M_{1120} = 184.79 \cdot \exp(-\omega/450.44) + 14.38$

Table 3. The mathematical relationships between rotational speed (ω) and tool temperature (T_p) at constant travelling speed (v).

No.	v [mm/min]	Models
1	112	$T_{p112} = 193.61 + 0.58 \cdot \omega$
2	224	$T_{p224} = 160.71 + 0.03 \cdot \omega$
3	560	$T_{p560} = 60.11 + 0.03 \cdot \omega$
4	710	$T_{p710} = 62.45 + 0.02 \cdot \omega$
5	900	$T_{p900} = 59.44 + 0.02 \cdot \omega$
6	1120	$T_{p112} = 51.85 + 0.01 \cdot \omega$

The opposite trend can be observed for changes in travelling speed (Fig. 7). Increasing the travelling speed causes an increase in the torque. This phe-

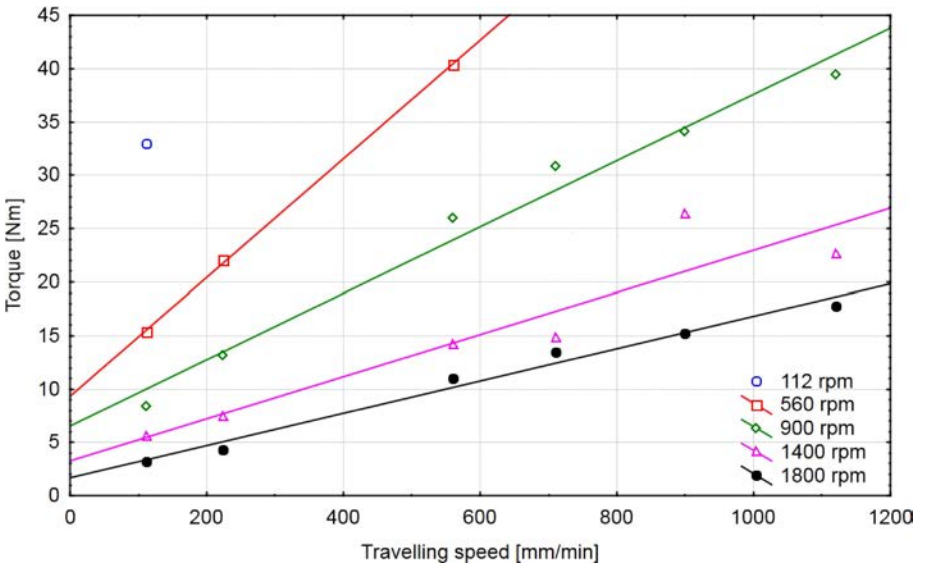

FIG. 7. The influence of the travelling speed on the torque acting on the tool at constant rotational speed.

nomenon is caused by the temperature changes during changes in the travelling speed. If the travelling speed increases, the total volume of stir material for each distance of linear travel of the tool decreases, so that small heat is generated. The temperature in the tool, therefore, becomes lower (Fig. 8). At low temperature the friction coefficient is high and the torque is higher for higher travelling

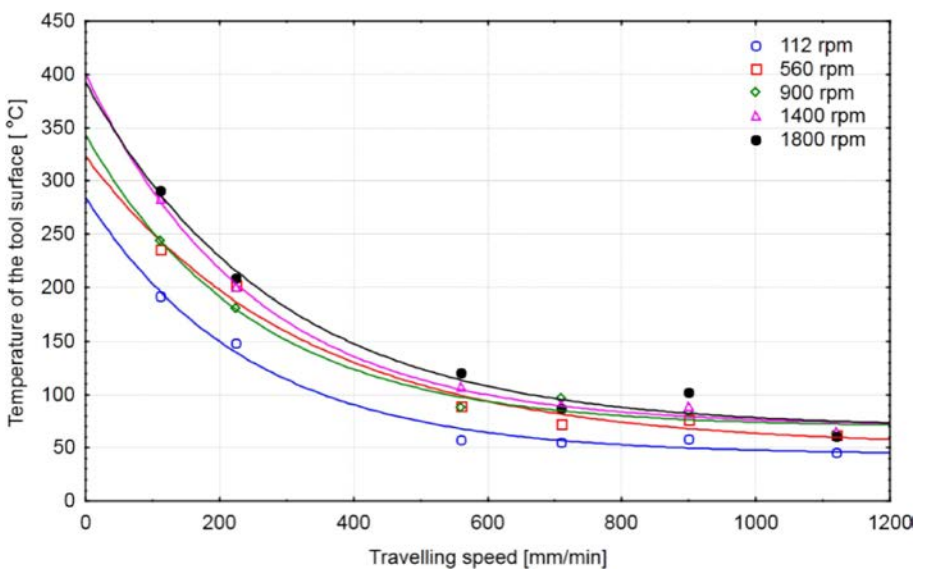

FIG. 8. The influence of travelling speed on tool temperature at constant rotational speed.

speeds. If the travelling speed is low, for single distance of travel the total volume of stir material is high so that the heat generated in the material is high. The temperature, therefore, is also high and the friction coefficient is lower. Hence the torque becomes lower. A linear formula has been found to describe the relationship between torque and travelling speed. The effect of travelling speed on the temperature of the modified material was successfully approximated by exponential functions. The results of mathematical modelling for torque and for temperature are given in Tables 4 and 5, respectively.

Table 4. The mathematical relationships between travelling speed (v) and torque acting on the tool (M) at constant rotational speed (ω).

No.	ω [rpm]	Models	Remarks
1	112	The mathematical formula cannot be determined because of too small number of measurements point	
2	560	$M_{560} = 9.36 + 0.06 \cdot v$	
3	900	$M_{900} = 6.53 + 0.03 \cdot v$	
4	1400	$M_{1400} = 3.26 + 0.02 \cdot v$	
5	1800	$M_{1800} = 1.71 + 0.02 \cdot v$	

Table 5. The mathematical relationships between travelling speed (v) and tool temperature (T_p) at constant rotational speed (ω).

No.	ω [rpm]	Models
1	112	$T_{p112} = 240.90 \cdot \exp(-v/243.53) + 43.86$
2	560	$T_{p560} = 272.02 \cdot \exp(-v/322.94) + 51.35$
3	900	$T_{p900} = 274.35 \cdot \exp(-v/247.36) + 69.28$
4	1400	$T_{p1400} = 330.36 \cdot \exp(-v/246.58) + 70.73$
5	1800	$T_{p1800} = 324.15 \cdot \exp(-v/283.23) + 68.68$

3.2. Results of metallographic examination

A representative light microstructure of the modified material is shown in Fig. 9. Two well defined regions can be easily distinguished: the parent material (lower area) and the FSP zone (upper area). The parent material is characterized by a coarse grain structure while the microstructure in the processed zone is modified by the tool action. The modified area resulted in the refinement of the microstructure. Figure 9 shows a region closer to the surface where the microstructure changes in a continuous way from that typical of the parent material to the refined one adjacent to the surface.

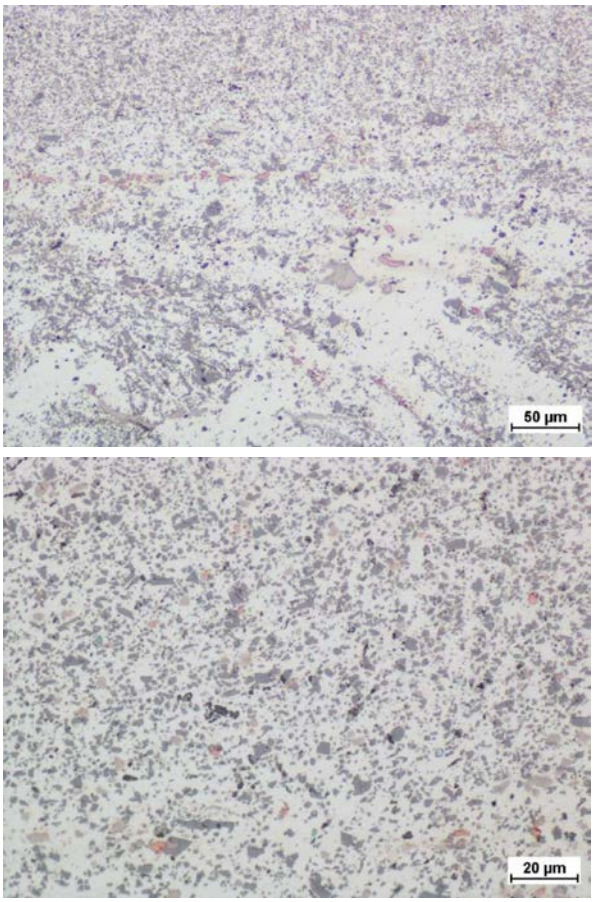

FIG. 9. A representative light microstructure of the FSP modified material – aluminium alloy AlSi9Mg.

High plastic deformation and material flow caused by the stirring action of the tool together with increased temperature due to friction phenomena are responsible for the refinement of grains and dynamic recrystallization in the modified area [14]. FSP also reduced casting pores and caused homogenization of the microstructure. As a result of FSP the as-cast material is converted into a near-wrought condition. This homogenized and refined microstructure along with the reduced porosity results in improved mechanical properties [15, 16]. It is also evident from the present study that the dramatic change in microstructure occurs even when a tool without a pin is used during FSP.

3.3. Modelling of the FSP process

Adapted from the friction stir welding thermal model presented by Hamilton et al. in [17], a thermal model was developed for friction stir processing utiliz-

ing COMSOL multi-physics software. As an initial simplification to the model, only heat generation due to the friction between tool and the workpiece was considered, i.e. heat generation due to plastic deformation was not taken into account. Based upon these conditions, the heat generation at the tool/workpiece interface, q, may be expressed as [17]:

$$q = \delta_E \mu P_N (\omega r - v_x \sin\theta), \tag{3.1}$$

where δ_E is an energy-based slip factor, μ is the coefficient of friction between the tool and the workpiece, P_N is the normal pressure relative to the tool face, ω is the angular velocity of the tool, r is the radial distance measured from the tool center, v_x is the tool velocity and θ is the radial angle measured about the tool axis.

For typical tool velocities during friction stir welding, the $v_x \sin\theta$ term in Eq. (3.1) becomes small relative to the ωr term and is often ignored. For the FSP process, however, the magnitude of certain tool velocities that were utilized, such as 900 mm/min and 1120 mm/min, makes the $v_x \sin\theta$ term non-negligible. Therefore, Eq. (3.1) was evaluated with $\theta = 90°$, and the heat generation was averaged over the tool/workpiece interface to yield the following expression for the tool heat flux, q_{tool}:

$$q_{tool} = \frac{\int_0^{r_{\text{interface}}} \delta_E \mu P_N (\omega r - v_x) r \, dr \, d\theta}{\pi r_{\text{interface}}^2} = \delta_E \mu P_N \left(\frac{2}{3} \omega r_{\text{interface}} - v_x \right), \tag{3.2}$$

where $r_{\text{interface}}$ is the radius of the tool face in contact with the workpiece. Basically, the FSP process stabilizes after approximately 10 seconds of runtime [18]. Prior to stabilization, the vertical force (as well as the torque) increases approximately linearly during the ramping period. Since the heat flux is directly proportional to the vertical force, a linear ramp for the heat flux was incorporated into the thermal model such that for runtimes less than or equal to 10 seconds ($t \leq 10$), the heat flux utilized in the thermal model, q_{model}, is given by:

$$q_{\text{model}} = \left(\frac{q_{\text{tool}}}{10} \right) t. \tag{3.3}$$

Beyond 10 seconds, i.e. after stabilization, the heat flux from Eq. (3.2) was used in the model.

In the first step the influence of pitch (rotational speed/travelling speed) on temperature at constant travelling speed was determined. Four numerical simulations were performed at a constant travel speed of 224 mm/min for the

following tool rotation speeds: 560, 900, 1400 and 1800 rpm. The predicted maximum surface temperatures for these simulations are summarized in Fig. 10. Included in the figure are the experimentally measured surface temperatures. As seen in the figure, though the predicted surface temperatures follow the same trend as the experimental values relative to the pitch, the thermal model under-predicts the processing temperature for the largest pitch (slowest rotation speed) and over-predicts the temperature for the two smallest pitches (the highest rotation speeds). The inability of the model to accurately predict the temperature at the highest pitch is most likely due to the fact that the thermal model does not presently capture heat generation due to plastic deformation. At slower rotation speeds, the processing energy transferred into the workpiece is reduced; therefore, the flow stress of the workpiece remains relatively high. As such, plastic deformation significantly contributes to the total heat generation.

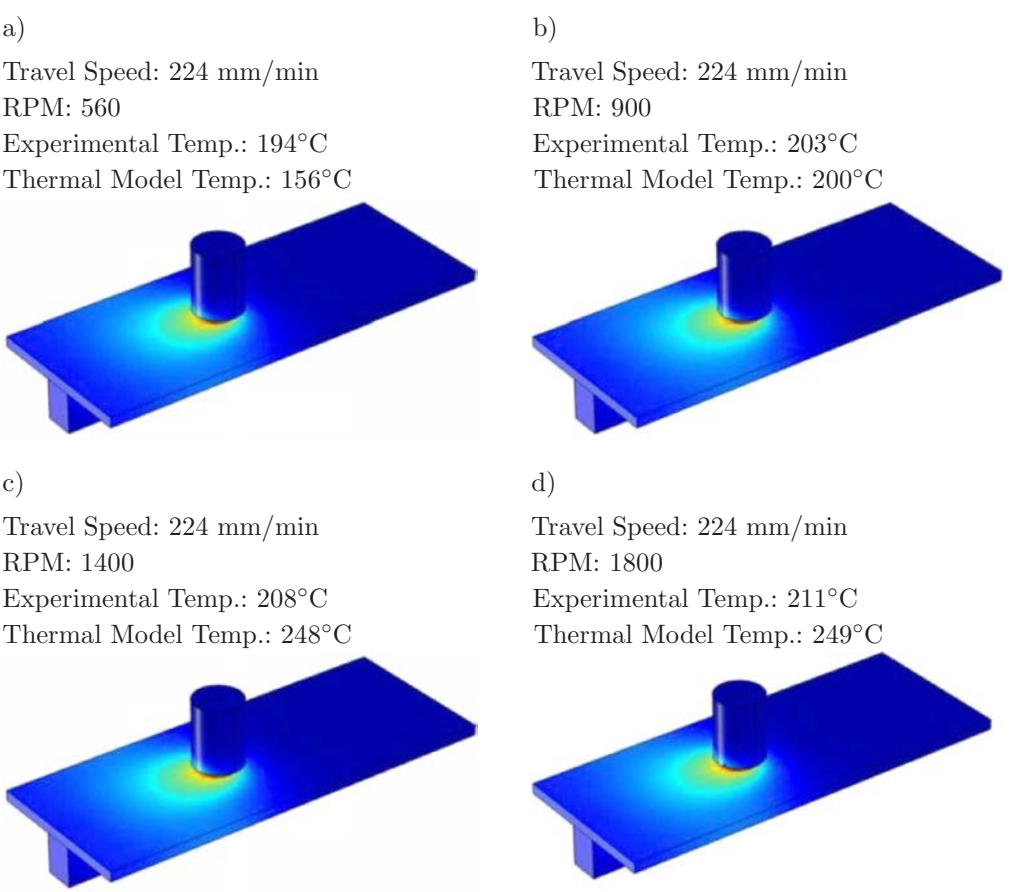

FIG. 10. Influence of pitch on temperature at constant travel speed: a) 0.4, b) 0.25, c) 0.16, d) 0.12.

The temperature over-predictions by the model at smaller pitches may be related to the slip factor, δ_E, utilized to calculate the heat flux (Eq. (3.1)). As previously discussed, the current model for FSP was adapted from a thermal model for friction stir welding for which δ_E represents the efficiency of frictional heat transfer. During friction stir welding, both a pin that is inserted into the workpiece and a shoulder that is in contact with the workpiece transfer frictional heat into the system, creating three heat generating surfaces: the pin bottom, the pin sides and the tool shoulder. During FSP, however, there is only one heat generating surface – the interface between the tool and the workpiece. The heat transfer during FSP, therefore, may be less efficient than during friction stir welding and is not accounted for by the current formulation of δ_E. For processing conditions for which heat generation due to friction dominates, such as at smaller pitches, the thermal model over-predicts the surface temperatures.

Secondly the influence of pitch on temperature at constant rotational speed was established. Six numerical simulations were performed at a constant rotational speed of 900 rpm for the following tool travelling speeds: 112, 224, 560, 710, 900 and 1120 mm/min. The predicted maximum surface temperatures for these simulations are summarized in Fig. 11. Included in the figure are the experimentally measured surface temperatures. As indicated in this figure for this rotational speed and associated travelling speeds, the experimental temperatures decline from approximately 250°C for pitch values less than 0.2 and then level off at approximately 100°C for pitch values greater than 0.8. Unfortunately, the thermal model failed to capture this experimental behaviour. Instead, the thermal model predicts that the surface temperatures for these conditions should begin at approximately 190°C for a pitch value of 0.12, rise to a maximum temperature of nearly 250°C at a pitch of 0.62, and ultimately fall to 145°C for the highest pitch value of 1.24.

Certainly the limitations of the model discussed in the previous section regarding heat generation due to plastic deformation and the slip factor can contribute to the discrepancies observed for these process conditions. In this instance, however, the effect of travel speed may be the primary cause for the discrepancies. Equation (3.2) captures the effect of travel speed in the $(\omega r - v_x)$ term, reducing the heat flux as the travel speed increases. This equation, however, assumes that the heat generating surfaces of the tool are in perfect contact with the workpiece. At travel speeds typical to friction stir welding, such as 127 mm/min, this assumption is undoubtedly valid. As the travel speed increases to values like those used in this investigation, such as 900 mm/min or 1120 mm/min, the efficiency of heat transfer from the tool to the workpiece could be reduced by the influence of these speeds on the tool/workpiece interface. As a result, the thermal model over-predicts the surface temperatures for these process conditions as the pitch increases.

a)
Travel Speed: 112 mm/min
RPM: 900
Experimental Temp.: 250°C
Thermal Model Temp.: 186°C

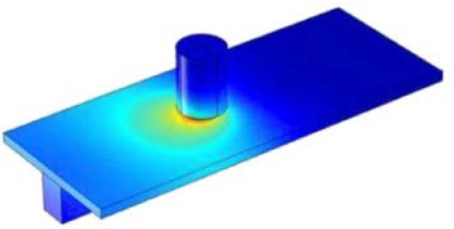

b)
Travel Speed: 224 mm/min
RPM: 900
Experimental Temp.: 203°C
Thermal Model Temp.: 200°C

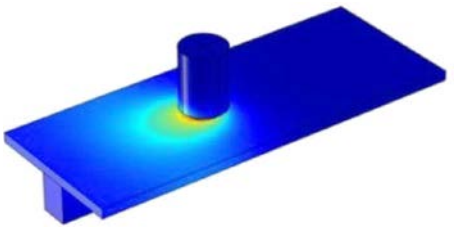

c)
Travel Speed: 560 mm/min
RPM: 900
Experimental Temp.: 140°C
Thermal Model Temp.: 247°C

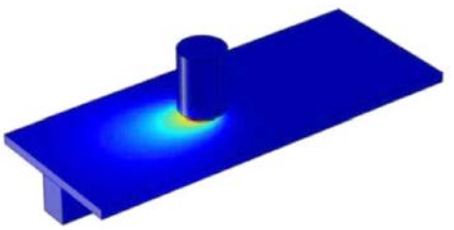

d)
Travel Speed: 710 mm/min
RPM: 900
Experimental Temp.: 100°C
Thermal Model Temp.: 219°C

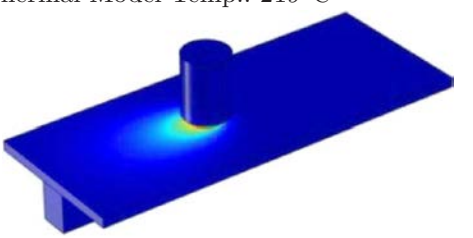

e)
Travel Speed: 900 mm/min
RPM: 900
Experimental Temp.: 100°C
Thermal Model Temp.: 177°C

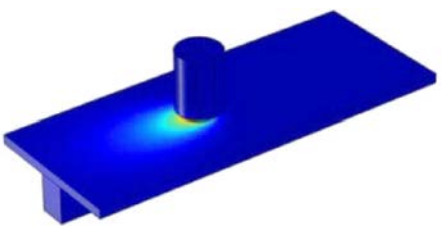

f)
Travel Speed: 1120 mm/min
RPM: 900
Experimental Temp.: 100°C
Thermal Model Temp.: 145°C

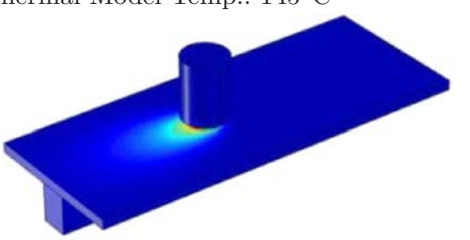

FIG. 11. Influence of pitch on temperature at constant rotational speed: a) 0.12, b) 0.25, c) 0.62, d) 0.79, e) 1.00 and f) 1.24.

4. CONCLUSIONS

The effects of rotational and travelling speeds on the torque and temperature of the tool were investigated for FSP of cast aluminium plates using experimen-

tal techniques and numerical modelling. The simulated temperatures were compared to measured values. From the simulation and experiments, the following are observed:

- The torque decreases with an increase in the rotational speed because it becomes easier for the material to flow at higher temperatures and strain rates. For an increasing temperature of the surface, the friction coefficient becomes lower. This is also due to the well-known relationship, from the conventional friction welding, that an increase in the rotational speed decreases the volume of mixed material.
- Changes in travelling speed influence the torque and temperature in opposite directions. An increase in the travelling speed decreases the temperature and increases the torque acting on the tool. This is due to the fact that an increase in the travelling speed raises the resistance of mixed materials, and a much higher volume of material is mixed per tool revolution.
- It is also evident from the present study that a dramatic change in the microstructure occurs, even when a tool without a pin is used during FSP. The modification process resulted in a significant breakup of large Si particles and subsequent uniform distribution in the aluminium matrix. Furthermore, porosity in the as cast AlSi9Mg was nearly eliminated by FSP.
- In the presented numerical model only heat generation due to the friction between tool and the workpiece was considered. The limitations of the presented model regarded heat generation due to plastic deformation and the slip factor. The influence of pitch on temperature at constant travelling and rotational speeds was determined. As a result, the thermal model over-predicts the surface temperatures for these process conditions as the pitch increases at constant rotational speed. At constant travelling speed the experimental and modelling results correspond.

Acknowledgment

The authors would like to thank the Ministry of Science and Higher Education in Poland for founding this work and Miami University for the support of our investigations.

References

1. Thomas W.M., Nicholas E.D., Needham J.C., Much M.G., Templesmith P., Dawes C.J., GB Patent Application No 9125978.8, 1991.
2. Mishra R.S., Ma Z.Y., *Friction stir welding and processing*, Materials Science and Engineering R: Reports, **50**, 1–2, 1–78, 2005.
3. Threadgill P.L., Leonard A.J., Shercliff H.R., Withers P.J., *Friction stir welding of aluminium alloys*, International Materials Review, **54**, 2, 49–93, 2009.

4. Mishra R.S., Mahoney M.W., *Friction stir welding and friction stir processing*, ASM International, Materials Park (Ohio) 2007.

5. Hamilton C., Dymek S., Blicharski M., *Mechanical properties of Al 6101-T6 welds by friction stir welding and metal inert gas welding*, Archives of Metallurgy and Materials, **52**, 1, 67–72, 2007.

6. Ma Z.Y., *Friction Stir Processing Technology – A review*, Metallurgical and Materials Transactions A, **39 A**, 3, 642–658, 2008.

7. Arora A., Nandan R., Reynolds A.P., DebRoy T., *Torque, power requirement and stir zone geometry in friction stir welding through modeling and experiments*, Scripta Materialia, **60**, 1, 13–16, 2009.

8. Khandkar M.Z.H., Khan J.A., *Prediction of temperature distribution and thermal history during friction stir welding: input torque based model*, Science and Technology of Welding and Joining, **8**, 3, 165–174, 2003.

9. Colegrove P.A., Shercliff H.R., *Two-dimensional CFD modelling of flow round profiled FSW tooling*, Science and Technology of Welding and Joining, **9**, 6, 483–492, 2004.

10. EN 1706:2010 Aluminium and aluminium alloys – Castings – Chemical composition and mechanical properties.

11. Cui S., Chen Z.W., Robson J.D., *Interrelationships among speeds, torque and flow volumes during friction stir welding/processing*, 8th International Friction Stir Welding Symposium, 18–20 May 2010, Timmendorfer Strand, Germany.

12. Lebiediev W.K., Ciernienko I.A., Wilija W.I., *Friction welding – handbook* [in Russian: *Svarka Treniem. Spravocnik. Izdatelstwo Maszinostronije*], Leningrad 1987.

13. Pilarczyk J., Pietras A., *Mechanism of heat release and propagation during friction welding of high speed to constructional steels*, International Conference Welding and Related Technologies for the 21st Century, Kiev Ukraine, 1998.

14. Karthikeyan L., Senthilkumar V.S., Balasubramanian V., Natarajan S., *Mechanical property and microstructural changes during friction stir processing of cast aluminum 2285 alloy*, Materials and Design. **30**, 6, 2237–2242, 2009.

15. Mahmoud T.S., Gaafer A.M., Khalifa T.A., *Effect of tool rotational and welding speeds on microstructural and mechanical characteristics of friction stir welded A319 cast Al alloy*, Materials Science and Technology, **24**, 5, 553–559, 2008.

16. Jayaraman M., Sivasubramanian R., Balasubramanian V., Babu S., *Influences of process parameters on tensile strength of Friction Stir welded cast A319 aluminium alloy joints*, Metals and Materials International, **15**, 2, 313–320, 2009.

17. Hamilton C., Dymek S., Sommers A., *A thermal model of friction stir welding in aluminum alloys*. International Journal of Machine Tools & Manufacture, **48**, 1120–1130, 2008.

18. Węglowski M.St., *An experimental study on the Friction Stir Processing process of aluminium alloy*. Key Engineering Material, 2013 in print.

Received December 5, 2012.